



The realisation of an electro-Optical Diffraction Grating using HeNe laser

Abdulsattar A. Aesa¹, C.D. Walton²

¹ Department of Physics, College of education-Alhaweja, University of Kirkuk, Kirkuk, Iraq.

² School of Mathematics and Physical Sciences, University of Hull, UK.

<https://doi.org/10.25130/tjps.v25i3.254>

ARTICLE INFO.

Article history:

-Received: 14 / 1 / 2020

-Accepted: 20 / 4 / 2020

-Available online: / / 2020

Keywords: Electro-optics effect, Liquid crystal, electro-Optical Diffraction Grating

Corresponding Author:

Name: Abdulsattar A. Aesa

E-mail:

abdulsattar_aesa2001@yahoo.com

Tel:

ABSTRACT

This paper reports far-field of the electro-optical diffraction grating to the advantage of electro-optic response of 5CB liquid crystal. The diffraction grating was produced by intersacting of two laser beam of laser HeNe 632.8nm wavelength radiation transmitted through a 5CB liquid crystal dopped Sudan Black B (SBB) dye in a cell with a thickness of 5 μ m and applying a uniform electric filed across the cell. Different concentrations of SBB dye were prepared and optically characterised. Double side tape in a thickness of 5 μ m was used to determine the cell thickness. Zero and two diffraction orders were observed. 16 μ m grating period involve in a produced electro-optical diffraction grating. The effect of changing voltage was investigated. The possibility of realising the electro-optical diffraction grating made of 5CB liquid crystal doped biocompatible material chitosan doped SBB dye to enhance the absorption properties were also investigated and characterised using Atomic Force Microscopy (AFM), Scanning Electron Microscopy (SEM), UV-vis spectrophotometer and optical microscope. A fabricated Electro-Optic diffraction grating was experimentally characterized. Applications of liquid crystal and the electro-optic effect were discussed briefly.

1. Introduction

The use of organic electro-optic material for electro-optical applications was suggested many years ago. Many devices have been developed since then, but some of them have been examined for their electro-optic response. [1]. Recently, there are some benefits of electro-optic polymers such as; producing high performance and low manufacturing costs. Examples of uses for these materials are a variable optical attenuator, as an electro-optic modulator or as an adjustable filter [2,3]. Such advantages allow the use of these materials in various applications such as optical devices [4], optical sensing [5], analog and digital signal processing and processing of information. The main idea of the electro-optics systems is to change the optical properties by controlling the applied voltage [6]. These materials have optical properties; the permittivity tensor and the refractive index vary. This means that when the light wave propagates through the electro-optic systems, they change some of the light characteristics such as direction, amplitude and frequency. Another reason for using the electro-optic field is waveguide

devices [7,8]. With a high speed of signal processing and communication network, this type of devices based on non-linear polymers have high performance and potential. The thin film's multi-layer structure can be used to create polymer optical devices, This is accomplished by beginning with a glass, silicon or upper electrode substratum containing precious metals such as silver and gold. This research investigated the electro-optical effect of a Polymer Dispersed Liquid Crystal (PDLC), 5CB liquid crystal (LC) doped with chitosan and doped with dye. This effect was used to construct a PDLC (5CB doped with chitosan) electro-optic diffraction grating doped with SBB dye. Polymer Dispersed liquid crystals (H-PDLCs) were fabricated with Switchable holographic grating using a 532 nm wavelength Argon laser [9]. This reported various grating periods made of solid PDLC films and was monitored in ± 2 diffraction order and higher. The PDLC has been utilised to create holographic transmissions and reflection gratings [10]. A HeNe laser was used to produce a phase hologram on a number of photopolymers and

3000 line mm^{-1} was obtained [11] also, the sensitivity of the diffraction grating was discussed. A refractive index grating was fabricated on the 5CB nematic liquid crystal doped with Sudan Black B (SBB) dye using HeNe laser and five diffraction orders were obtainable [12]. Ar laser was used to make a quasi-permanent grating on a 5CB photorefractive nematic liquid crystal doped with a fullerene (C60) [13]. In addition, nematic liquid crystal 5CB diffraction gratings, doped with a Norland polymer using a HeNe laser, have been reported [14]. Nematic LC E7 doped with azo dye was produced with a polarization grating using a holographic system with a CW Ar laser operating at 488 nm wavelength [15]. It was verified that the grating period was 15 μm . Using a diode-pumped-solid-state (DPSS) laser operating at a wavelength of 532 nm, a diffraction grating was developed on a LC E7 doped m film with methyl red (MR) dye [16].

Furthermore, liquid crystals in a nematic phase (NLCs) have an effect on their optical properties by the electrical field [17]. William has studied the first experiment in this area [18]. Liquid Crystals (LCs) display three phases known as the; smectic A, nematic and isotropic phase [19] as shown in Fig. (1). it can be noticed that increasing the temperature changes the LC phase: some of them exhibit a nematic phase at low temperature matrices, while at high temperature others exhibit a isotropic phase namely Smectic A.

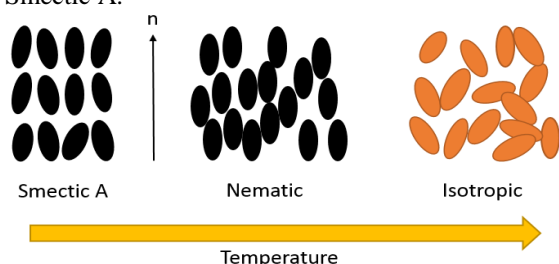


Fig. 1: Picture of the liquid crystal phases shows the orientation order in the Smectic A, Nematic and isotropic phases [19].

A liquid crystal (LC) material that has drawn great attention is the 5CB (4-n-pentyl-4'-cyanobiphenyl). The simple molecular structure of 5CB undergoes a nematic phase transition at room temperature [20]. Fig. (2) shows the chemical structure of the 5CB LC. This property allows it to be used for physical behaviour investigations for a simple nematic material [21]. The 5CB liquid crystal has offered excellent physical and chemical properties such as chemical stability, stable mesophases, optical anisotropy and high dielectric properties. However, the absorption of the visible light range is weak [22]. The properties of the thermotropic liquid crystal 5CB make it suitable for a wide range of applications such as optoelectronics [23], storage technologies [24,25] and for visual displays [18].

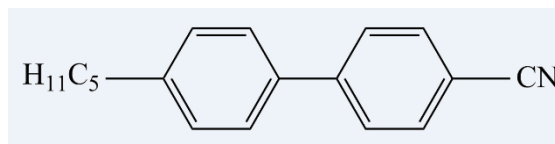


Fig. 2: The chemical structure of 5CB liquid crystal produced by using chem. office.

There has been a lot of interest in polymer dispersed liquid crystals (PDLCs) films in the last few years. Such films consist of microdroplets of liquid crystal dispersed within the polymer matrix [26]. When using an electrical field, the PDLCs give controllable optical properties. By varying the strength of the electrical field, there are noticeable changes in the properties of light dispersion as the composite changes to a transparent property [27]. PDLCs have been used for various applications such as a holographic grating light window, switchable displays and as an optical attenuator (VOA) [28–30]. In addition, liquid crystals doped with dye have received a lot of attention from research groups. Changing the non-linear optical properties of liquid crystals is perhaps the most important effect of dye molecules on the LC [31]. The non-linear optical behaviour of dye-doped liquid crystals is influenced by various parameters such as dye concentration, temperature, intensity and laser wavelength [32]. Sudan Black B (SBB) is an azo-dye has been widely used for doping LCs and this dye was used in this work.

The Sudan Black B (SBB) azo-dye was developed by Lison in 1934 as a specific lipid stain [37]. Lison states that biologically derived lipids can be used to remove the Sudan Black B dye. In addition, various solvents such as acetone-alcohol, propylene glycol, ethyl alcohol and ethylene glycol have been used to dissolve SBB. The chemical structure of the SBB dye is shown in Fig. (3) [31]. Some of the advantages of using the SBB dye are its high stability and high dichroic ratio due to its rod-like molecular form.

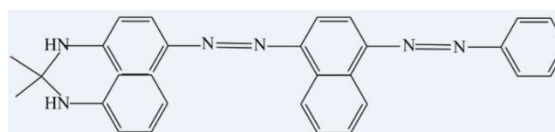


Figure 3: The chemical structure of Sudan Black B (SBB) produced by using chem. office.

1.1. Fredericksz transition

In 1933, the Russian physicist, Vsevolod Fredericksz, first investigated the Fredericksz Transition (FT) [38]. In the molecular alignment of liquid crystals, a *phase transition* occurs when either an electrical or magnetic field is applied. The LC molecules continue to interact with the electrical field when a liquid crystal (LC) material is placed between two parallel plate electrodes and an electrical field is applied. The molecules are paired just above a certain level of voltage / electric field. This threshold is called the Fredericksz Transition (FT) and because of its freedom of movement, it is a unique property of

liquid crystal materials [33]. It was reported that when a magnetic field is applied, molecular orientation can also be observed [34] But we are mainly interested in responding of the LC molecules when an electrical field is applied. The equation below is used to determine the FT threshold caused by an electrical field [35]:

$$E_{th} = \frac{\pi}{d} \sqrt{\frac{K_{11}}{\epsilon_0 \Delta \epsilon}} \dots (1)$$

where d , K_{11} , ϵ and $\Delta \epsilon$ are the cell thickness, elastic constant, the electrical permittivity of free space and dielectric anisotropic respectively. Then the equation below can be used to determine the threshold voltage:

$$V_{th} = E_{th} d \dots (2)$$

combining equations (1) and (2) we can write:

$$V_{th} = \pi \sqrt{\frac{K_{11}}{\epsilon_0 \Delta \epsilon}} \dots (3)$$

The elastic constant K_{11} can be determined with knowledge of threshold voltage, electrical permittivity and dielectric anisotropic parameter. We will later evaluate K_{11} experimentally and then analyze the experimental results. A schematic diagram of molecular alignment with and without an applied electrical field is shown in Fig. (4):

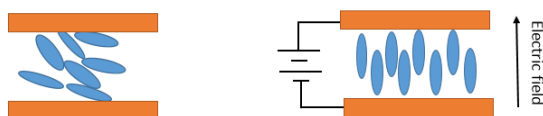


Fig. 4: Schematic illustration show in the effect of applying an electric field to a LC cell. When the electric field is applied as shown the director is oriented normal to the plane of the electrodes.

2. Methodology

2.1. The preparation of PDLC doped dye solution

5CB liquid crystal was collected from the School of Chemistry at the University of Hull, Kingston Chemicals Limited. The chitosan-doped 5CB LC procedure at different ratios has been described previously [36]. In our study, 5CB LC in the ratio of 2:8 was doped with chitosan. Chitosan solution was added to the 5CB LC by 2 percent (wt./v), the mixture was then put on a magnetic stirrer plate for 1 hour until the solution was milky. An azo-dye Sudan black B, (SBB) (Sigma Aldrich, 199664-25G, Lot # MKCD1338) has been used to increase laser light absorption. For each mass, the dye was dissolved in 10 mL of ethanol (0.01 mg, 0.02 mg, 0.03 mg, 0.04 mg, 0.05 mg, 1 mg, 2 mg) to achieve different concentrations (0.1, 0.2, 0.3, 0.4, 0.5, 1, 2) percent of wt./v respectively. Azo-dye Sudan black B (SBB) mixture was examined at concentrations of 2 percent in 5CB LC and 5CB PDLC doped with chitosan

2.2. Cell preparation

The PDLC doped with SBB dye cells were prepared to form transparent electrodes using two glass plate coated with Indium Tin Oxide (ITO) ($25 \times 25 \times 1.1$ mm). The ITO slides were bought from

(delta-technologies, USA, CG-81IN-0115, polished float glass, with an electrical resistance of 30-60 ohms on the ITO coated surface. Next, the ITO slides were cut into plate sizes (12×25 mm) and then cleaned. Every cell was prepared by using the PDLC solution doped with dye by sandwiching them. The cavity between the two plates was made by using an ultra-thin double-sided adhesive tape with a thickness of $5 \mu\text{m}$ obtained from (Nitto co, Nitto Denko UK Ltd). The cell preparation is shown in Fig. (5).

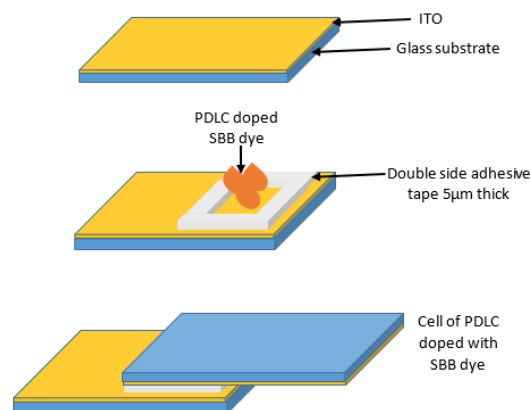


Fig. 5: The cell structure of PDLC doped with SBB dye.

An image of the electro-optical cell used in the experiments is shown in Fig. (6). The design of cells is being discussed. Using silver dag, the wires shown in this figure were attached to apply the electrical field.



Fig. 6: The cell of PDLC (5CB doped with chitosan) doped with SBB dye.

2.3. Realisation of the electro optical diffraction grating

The electro-optical diffraction gratings inscription experiment was conducted using a holographic set-up, see Fig. (7). It consists of two lasers with a combined power output of 10 mW for the laser inscription and 1 mW for the laser probe beam. In order to create an interference fringe inside the PDLC doped with SBB dye cell, a cubic beam splitter (Thorlabs) was used to split the laser beam. To guide and cross the converging laser beams, a mirror (Thorlabs, 25 mm diameter) was used. To achieve a P-polarized beam, two linear polarizers were used. The sample was placed on mechanical X, Y, Z stages

with orthogonal axes so that the appropriate interference pattern could be accurately controlled. To provide a voltage in the range of (0-30) V, a DC power supply was connected to the cell. After the cell a screen was mounted to monitor the diffraction instructions.

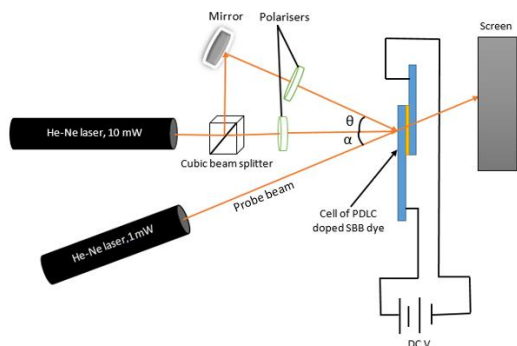


Fig. 7: The experimental set up for the realization of the electro optical diffraction grating made from a PDLC doped SBB dye.

The grating period of the interference pattern for the geometry of two beams shown in Fig. (7) can be determined by

$$d = \frac{\lambda}{2 \sin \theta} \dots(4)$$

where d is the grating period, λ is the wavelength of light and θ is the angle between two intersecting laser beams. The angle of the intersection has been modified in this experiment to be $= 1.2^\circ$. The angle α shown in this diagram is the probe beam's incident angle on the sample and is calculated to be $\alpha = 7.2^\circ$. From equation 7-5 it was determined that the grating period generated by interfering beams was $15 \mu\text{m}$. Cells of 5CB doped with SBB dye and PDLC doped with SBB dye at a thickness of $10 \mu\text{m}$ were illuminated with P-polarized write beams with a power of about 1.8 mW each.

3. Results and discussion

In this section, the results of all experiments will be presented and analyzed. Materials were used in all experiments are as follow; 5CB LC doped SBB dye and 5CB LC doped SBB dye doped chitosan.

UV-VIS measurements were performed on 5CB LC and 5CB LC chitosan doped solutions. Fig. (8) shows the absorption of 5CB LC and 5CB LC doped chitosan. It can be seen that in the ultraviolet and visible range the 5CB LC has relatively high absorption. As can be seen, at wavelengths $< 350 \text{ nm}$, optical absorption increases more. This figure shows similar behaviour in the absorption of PDLC and PDLC doped dye, but the chitosan sample shows a slightly stronger absorption at shorter wavelength.

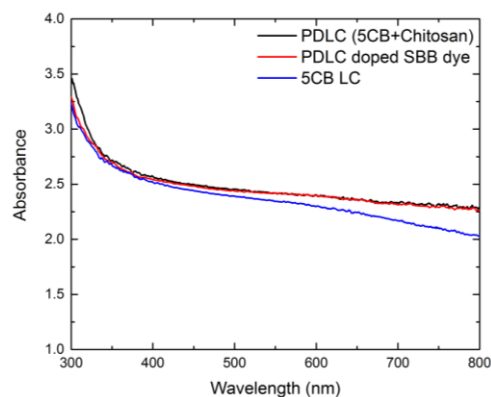


Fig. 8: The UV-VIS spectrum of the absorbance of 5CB LC solution (blue line), PDLC 1% (5CB LC doped chitosan, black line) and PDLC doped 0.5% SBB dye (red line).

UV-VIS absorbance of SBB at different concentrations (0.1%, 0.2%, 0.3%, 0.4%, 0.5%) wt. /v is shown in Fig. (9). It is clear that the SBB dye has nearly high absorption at the visible range by this figure and reaches the maximum absorbance intensity at a wavelength of 610 nm at approximately 0.6 for 0.5 percent and the lowest intensity at 0.1 percent at the same wavelength as the dye concentration rises. Although, at a wavelength of 420 nm , SBB dye has a significant absorption. SBB dye absorbs light in the visible range by promoting π orbital electrons from the earth to a higher energy level [37].

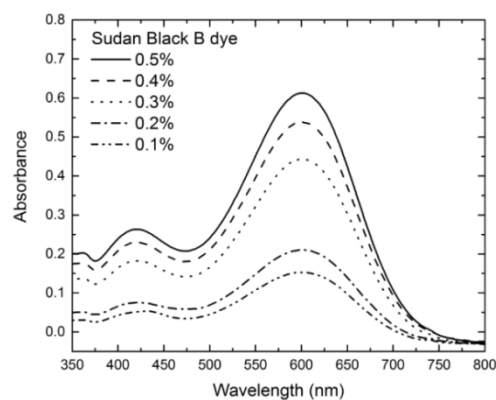


Fig. 9: The UV-VIS spectrum of Sudan black B (SBB) in different concentrations (0.1%, 0.2%, 0.3%, 0.4%, and 0.5%) wt. /v.

Using the Tauc relationship, a material's optical bandgap energy (E_g) can be obtained from the UV-VIS spectrum. The optical bandgap can be determined with knowledge of the absorption coefficient. The Tauc relationship can be written as follows [38].

$$\alpha = A \frac{(h\nu - E_g)^n}{h\nu} \dots(5)$$

Where α is the coefficient of absorption, A is constant, E_g is the energy of the bandgap, and n is 0.5 and 2 for the direct transition material and for the indirect transition material. The SBB dye's bandgap energy is determined using the $n = 0.5$ Tauc relationship as the SBB dye has a direct transition. Plots between $h\nu$ and $(\alpha h\nu)^2$ for different concentrations (0.1 percent, 0.3 percent, 0.5 percent) of SBB were performed to assess the bandgap energy and are shown respectively in Figs 10, 11 and 12. The absorption coefficient was determined using Beer's law ($\alpha = A/cb$) where A is the absorbance, c is the concentration and b is the path length of the medium inside the cuvette. Such figures show that the bandgap energy decreases as the dye concentration increases; 1.838 eV, 1.821 eV and 1.814 eV for 0.1%, 0.3% and 0.5% respectively.

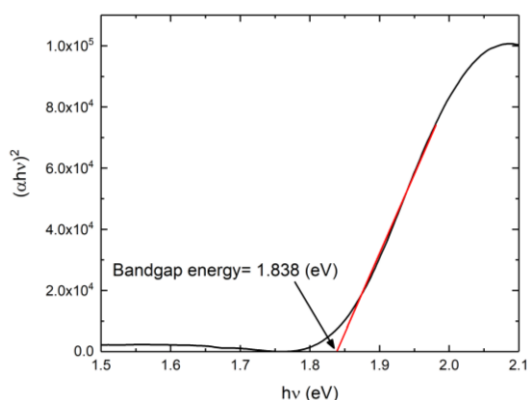


Fig. 10: The bandgap energy measurement of Sudan Black B dye in a concentration of 0.1% wt. /v using the Tauc relation.

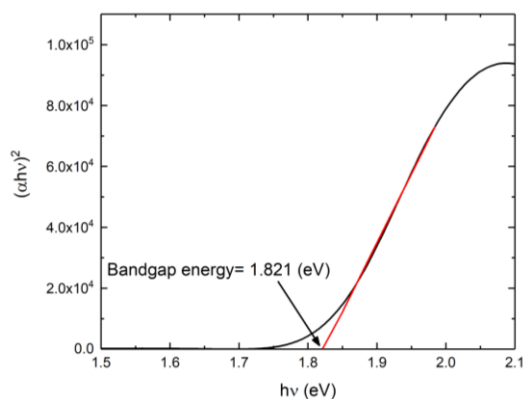


Fig. 11: The bandgap energy measurement of Sudan Black B dye in concentration of 0.3% wt. /v using the Tauc relation

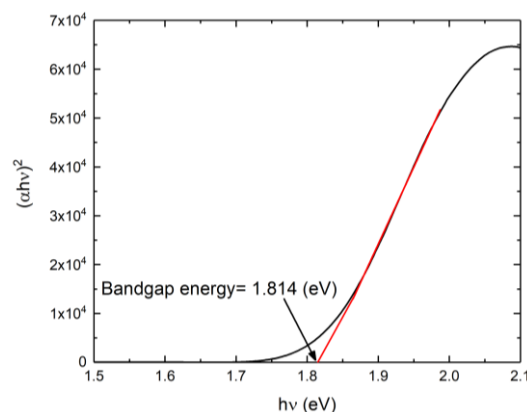


Fig. 12: The bandgap energy measurement of Sudan Black B dye in a concentration of 0.5% wt. /v using the Tauc relation.

Fig. (13) shows the optical micrographs of polymer dispersed LC's optical textures in the 20:80 (wt. percent) ratio (5CB: chitosan). Dispersed in the biopolymer chitosan matrix, optical microscopic images show a non-homogeneous distribution of 5CB LC. Such optical microscope images show the birefringence of the 5CB texture. The birefringence is one of the nematic LC materials' optical properties. The nematic LC displays the birefringence as the refractive index is influenced by the direction of light passing through the sample [22]. In addition, the birefringence shift is followed by a change in the liquid crystalline phase transition[45]. The nematic LC has a large birefringence that makes it ideal for viewing liquid crystal devices [22]. As well as an observation showing that in the biopolymer matrix the liquid crystal is distributed non-homogeneously. Fig. (13, B) indicates that the 5CB LC has organized like trees and these may be due to the phase of the coating. Fig. (14) displays AFM micrographs of 5CB LC randomly distributed molecules that support the observation in the optical micrographs.

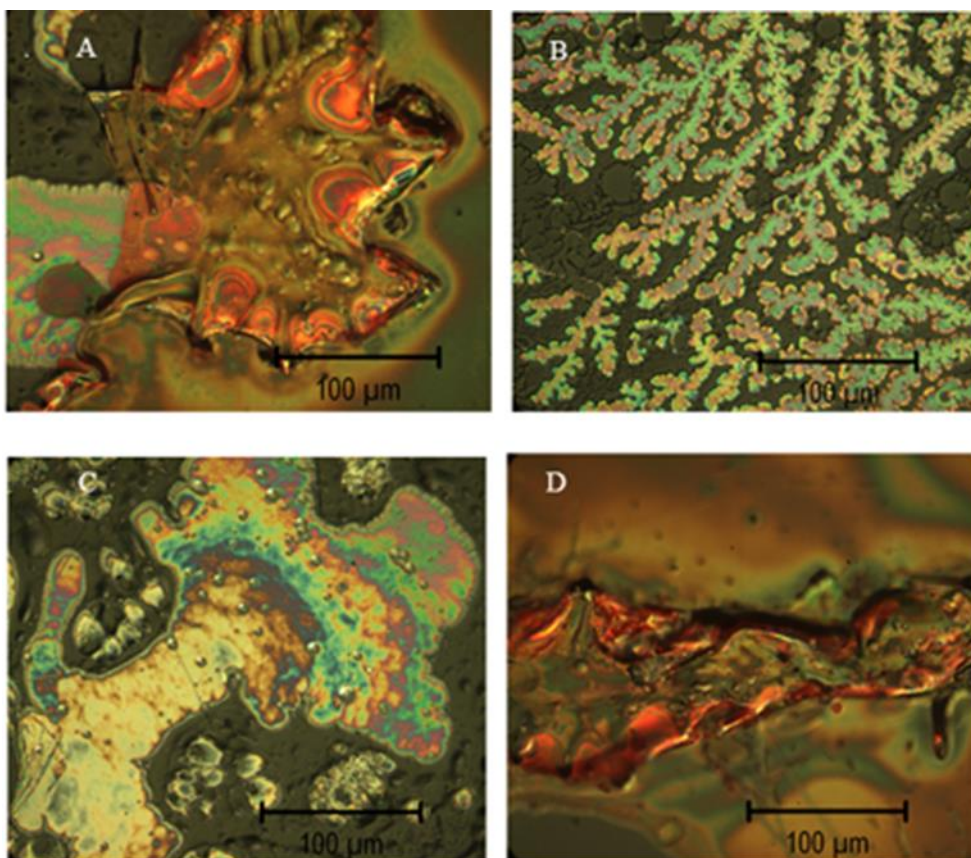


Fig. 13: (A, B, C and D) optical micrographs of 20:80 (wt. %) polymer dispersed liquid crystal 5CB doped with chitosan.

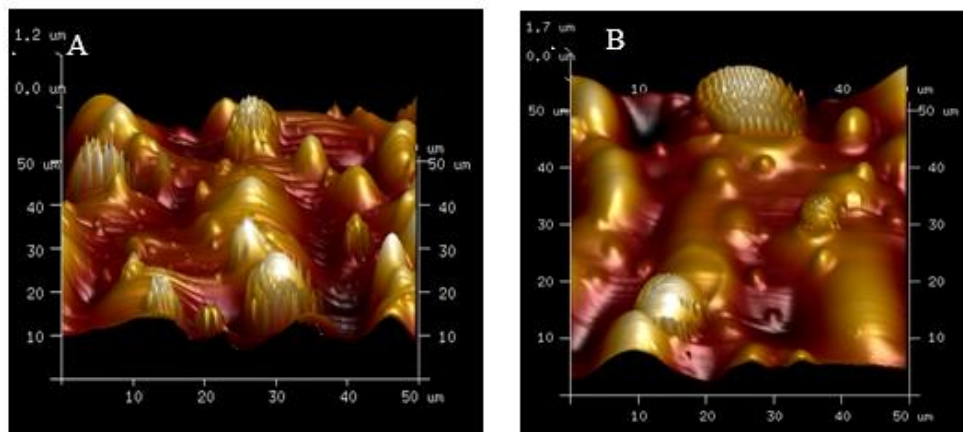


Fig. 14: (A and B) AFM micrographs of 20:80 polymer dispersed liquid crystal 5CB doped with chitosan.

Fig. (15) shows a He-Ne laser probe beam that is incident on a viewing screen after the light beam passed through the LC cell Fig. (14) containing 5CB LC doped with SBB dye. The cell cavity used in the experiment was 10 μm in length. A relatively small cavity length was chosen so that a large electric field could be applied at a small applied voltage. We note two effects in the figures that are of interest. In both figures A and B there are concentric rings forming around the central laser spot. In Fig. (15B) we observe diffraction orders, along a horizontal plane. The diffracted orders are formed by the grating that has been inscribed by the interference

of the overlapping HeNe writing beams. The ± 1 and ± 2 orders can be seen in the photograph. As can be seen, the intensity decreases with increasing diffraction order. We interpret the concentric rings as being due to the nonlinear response of the refractive index and the Gaussian spatial HeNe beam. On the application of an electric field, the rings were seen to vanish at 3 ± 0.1 Volts. This corresponds to an electric field strength of $3 \times 10^5 \text{ Vm}^{-1}$. Similar rings patterns have been previously seen in publications and are thought to be due to the Fredericksz transition [39] or due to a nonlinear effect [40].

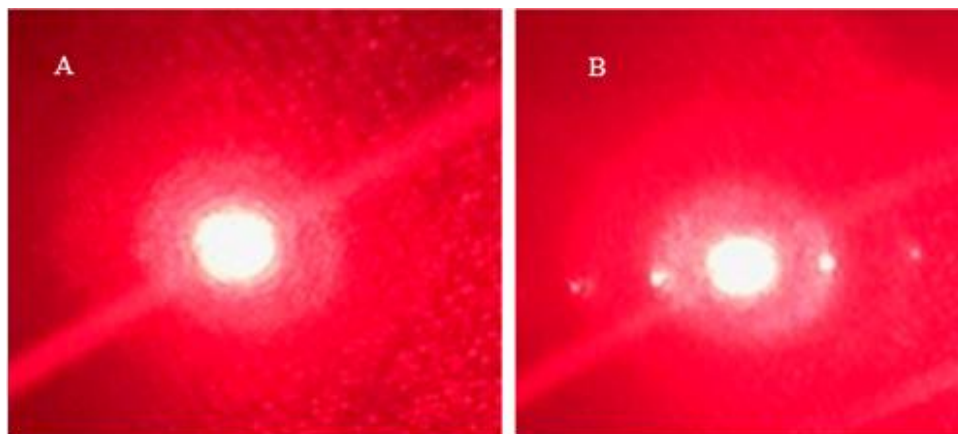


Fig. 15: Photographic images of the viewing screen showing concentric rings centred around the central HeNe laser probe beam. Both show a ring pattern produced when the cell is applied with 3 volts across the LC cell. (A) is shown without the HeNe intersecting writing beams. (B) has the same conditions as in (A) but with the addition of two interfering HeNe beams used for inscribing a grating inside the cell. One can observe in a horizontal direction the ± 1 and ± 2 diffraction orders. The cell thickness along the beam direction is $10 \mu\text{m}$.

The 5CB LC doped Freedericksz transition with SBB dye was measured $6.2 \text{ V}[10]$. For the $20 \mu\text{m}$ thick cell used in the experiment, this corresponds to an electrical field of $3.1 \text{ media}10^5 \text{ Vm}^{-1}$. This shows a good agreement with the acquired value in this work. At an electrical field of $5 \times 10^5 \text{ Vm}^{-1}$, the ring structure reached a maximum diameter and vanished when an electrical field was applied at $6 \times 10^5 \text{ Vm}^{-1}$ and above. The rings lasted for an additional 5 seconds before vanishing when the electric field was stopped. The ± 1 and ± 2 diffraction orders are located along an almost horizontal direction in Fig. (15B). Since switching on the HeNe intersecting grating inscribing beam, the diffraction instructions took place after 25 minutes. The grating period was measured using the experimental setup's ordered spacing and geometry and corresponded to a $16 \mu\text{m}$ grating period. This value has a good agreement with the grating period calculated by equation (4) which corresponded to $15 \mu\text{m}$. At an applied voltage of 5 V, the grating orders with the highest contrast were observed, corresponding to an applied electric field of $5 \times 10^5 \text{ Vm}^{-1}$. Due to the alignment of the LC molecules along the intervening fringes with higher intensity, the formation of the diffraction grating can be explained qualitatively.

The electric field application has the purpose of assisting the alignment as shown in the example Fig. (15). These two processes are referred to as the optical field and the electrical field. Turning our attention to the ring patterns around the HeNe probe beam. The power of the probe beam was 1 mW and had a typical Gaussian beam with a diameter of 1 mm. Therefore, the central on-axis part of the beam has the highest intensity. The refractive index of the LC is highly birefringent and its value is dependent on the laser beam intensity according to the relation ($\Delta n = n_2 I$), where $\Delta n = n_e - n_o$, n_e and n_o are the extraordinary and ordinary parts of refractive index respectively, n_2 are the nonlinear coefficient and I

correspond to the HeNe beam intensity. Therefore, a higher intensity will have a higher refractive index. Moreover, the refractive index will reach the highest value in the central portion of the Gaussian beam while out towards the wings of the Gaussian the refractive index decreases. Consequently, there is a change in the phase of the propagating wave and rings will form due to constructive and destructive interference occurring. In this experiment, there are therefore two processes taking place. Ring formation due to the spatial dependent refractive index and there is a grating formed due to the intersecting inscribing HeNe beam. From this information, we can calculate the birefringence (Δn) using the equation ($\Delta n = \frac{N\lambda}{d}$)

[40]. Using the corresponding information, where N is the number of observed rings the birefringence is calculated to be 0.126, λ is the wavelength 632.8 nm and d is the cell thickness which is $10 \mu\text{m}$. Similarly, rings patterns generated on the 5CB doped with methyl red dye (MR) as self-phase modulation (SPM) have been reported using Nd:YVO₂ laser operating at a wavelength of 532 nm [40]. The concentric rings represented by Fig. (15A and B) could back to Freedericksz transition in the liquid crystal molecules. This transition is a result of the contribution between the alignment of the molecules director at the surface and the boundary of the cell. The molecular director can be induced within the sample by applying a sufficient electric field or magnetic field [41]. Regarding the diffraction order represented by the dots in the Fig. (16B), these diffraction grating can be produced by irradiating the liquid crystal with polarized light. The optical field of the light impinging the sample controls the orientation of the liquid molecules to generate the phase grating of the liquid crystal material.

A set of experiments were carried out on PDLC doped with SBB dye with the aim of realising an electro-optic tunable diffraction grating the results of which are discussed.

Photographs of the images recorded on a viewing screen are shown in Fig. 16 (A and B): (A) the incident probe beam on the viewing screen after passing through the cell without the writing beam. (B) images on the viewing screen when the writing

beams are switched on for a cell of PDLC doped with SBB dye and with an applied electric field. There is some evidence of faint, low contrast circles around the incident probe beams for both images A and B.

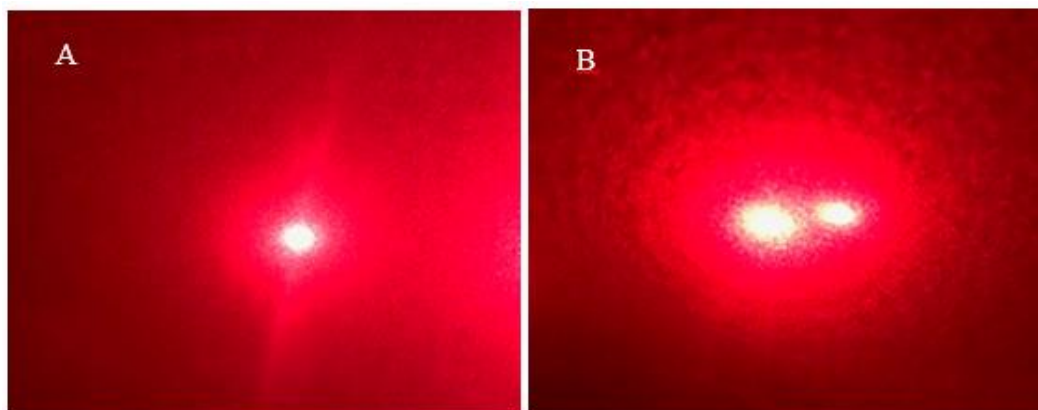


Fig. 16: (A) the incident probe beam on the viewing screen after propagating the cell containing PDLC (5CB doped with chitosan) and with doped with SBB dye. (B) The incident of writing beams on the viewing screen after propagating the cell. All these images were under applying an electric field. The thickness of the cell is 10 μm .

SEM micrographs of the surface of the PDLC (5CB doped with chitosan) doped with dye after probing with a HeNe, whilst applying an electric field are shown in Fig. 17 (A and B). It was observed that the suspension of PDLC doped dye had solidified and had a silver colour. However, it is not known if the changes were due to the interaction with the HeNe

laser, due to the application of the electric field or a combination of the two processes. It can be seen in Fig. 17 (A) there is also the appearance of cavities. The changes that have occurred to the material require more investigations to explain the related mechanism.

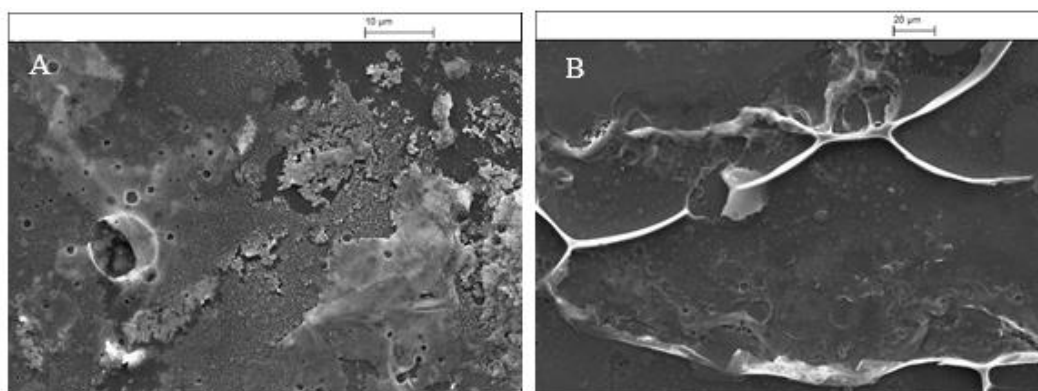


Fig. 17: SEM micrographs of the surface of PDLC doped with SBB dye after probing with a HeNe laser and applying an electric field. The sample thickness is 10 μm . A magnification of $\times 5$ was used, at a tilt angle of 0° , (B) $\times 1.5\text{K}$ magnification, and 0° tilt angle.

Fig. 18 (A and B) shows optical micrographs of PDLC doped SBB dye after probing the LC cell with a HeNe laser beam and applying an electric field across the material. It shows that there is a significant

change in the distribution of 5CB LC dispersed in the biopolymer matrix and optical textures of the mixture.

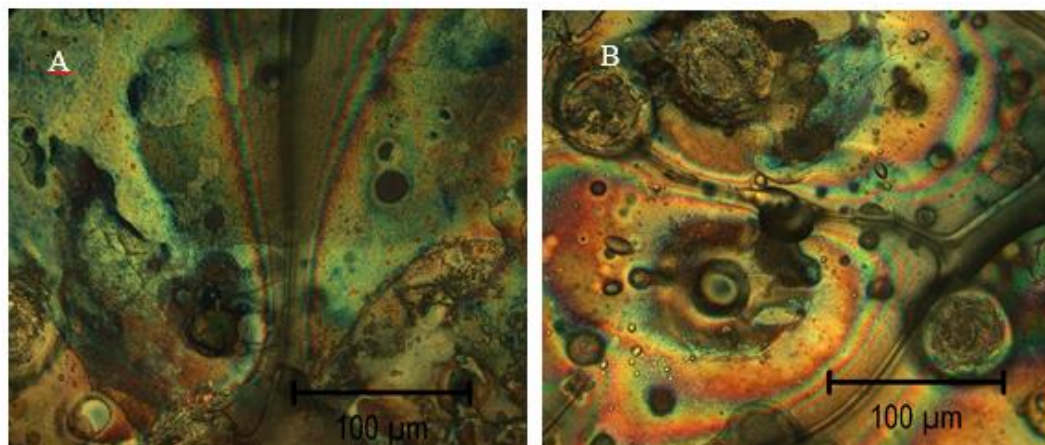


Fig. 18: Optical micrographs of PDLC (5CB doped chitosan) doped Sudan black B (SBB) dye after probing with HeNe laser and applying an electric field.

The next set of experiments were intended to have a 5CB doped with SBB mixed with chitosan. Previous work on chitosan doped 5CB reported the miscibility [36]. An experiment was performed using the same experimental conditions as the non-chitosan experiment previously described. However, the results did not yield a diffraction pattern and hence under the same conditions, we concluded a diffraction grating had not been inscribed.

As has been mentioned above that filling the cell in a thickness of 10 μm with the mixture of the PDLC doped chitosan and with SBB dye converted into a solid within a few minutes after interacting with the HeNe beams and applying a DC electric field. Although the refractive index and absorption coefficient were not measured and no values could be found in the literature it is expected that the optical properties for this set of experiments are different to the previous one that had no chitosan present. The optical penetration depth at 632.8 nm, the refractive index and elastic constant will all be different. All of which will play a role in inscribing a grating. This does not, however, conclude that it is not possible to inscribe a grating in 5CB doped with SBB and chitosan. It may be that different experimental parameters are required in order to realise a grating.

4. Conclusion

Although there are several ways of achieving an electro-optical diffraction grating, we have investigated an electro-optical method using a liquid crystal namely 5CB. In this work, we mixed Sudan Black B, (SBB) to increase the absorption of light at the inscription wavelength of 632.8 nm. This sample is identified as 5CB/SBB. A second sample was made by adding chitosan. This sample is therefore referred to as 5CB/SBB/Chitosan. Two sets of experiments were carried using these samples, 5CB/SBB and 5C/SBB/Chitosan. The former was used as a reference and the latter, to our knowledge, has not been reported in the literature. A HeNe laser beam

was split using a 50:50 cubic beam splitter and beams recombined to form interference fringes inside the samples. A set of experiments were carried out to investigate the effects of applying an electric field normal to the sample surface whilst the grating inscription process is taking place. From the geometry of the interfering HeNe laser beams, a fringe spacing of 15 μm was calculated. Light from a HeNe laser was switched on and an electric field of magnitude $5.1 \times 10^5 \text{ Vm}^{-1}$ was applied at the same time. After 25 minutes the ± 1 and ± 2 diffraction orders were observed on a viewing screen placed behind the sample. From these results, we conclude the addition of SBB increased the optical absorption at the wavelength 632.8 nm and aided in the formation of a diffraction grating. The experiment was then repeated using a different sample, namely 5CB/SBB/Chitosan.

It is also worth noting that the 5CB/SBB/chitosan sample solidified after the experiment. A separate experiment revealed solidification occurred under the same conditions after 15 minutes. However, the mechanism of solidification was not investigated. The solidification may be due to a combination of factors. The interaction of light from the HeNe interacting with the chitosan may change the material structure or it may be due to the miscibility between 5CB and SBB. Using the same experimental conditions as those used for the 5CB/SBB sample it was not possible to observe a diffracting structure. The ratio of 5CB/SBB/Chitosan used in the experiment was 1:4:8 respectively and further experiments using different ratio's of materials have been discussed for future experimental investigations.

Acknowledgement

We acknowledge the Ministry of Higher Education & Scientific Research, Iraq for supporting this work. Mr Anthony Sinclair is also acknowledged for the SEM measurements.

References

- [1] J.C. Bosshard, K. Sutter, R.S. and P.G. (1993) Electro-Optic Effects in Molecular Crystals. *Josa B*, **10**, (5), 867–885.
- [2] JGhasemi, F., Entezar, S.R. and Razi, S. (2019) Terahertz Tunable Photonic Crystal Optical Filter Containing Graphene and Nonlinear Electro-Optic Polymer. *Laser Physics*, IOP Publishing, **29**, (5).
- [3] JMiura, H., Qiu, F., Spring, A.M., Kashino, T., Kikuchi, T., Ozawa, M., Nawata, H., Odoi, K. and Yokoyama, S. (2017) High Thermal Stability 40 GHz Electro-Optic Polymer Modulators. *Optics Express*, **25**, (23), 28643.
- [4] Ye, C., Liu, K., Soref, R.A. and Sorger, V.J. (2015) A Compact Plasmonic MOS-Based 2x2 Electro-Optic Switch. *Nanophotonics*, **4**, (1), 261–268.
- [5] Taylor, H.F. (1987) Application of Guided-Wave Optics in Signal Processing and Sensing. *Proceedings of the IEEE*, **75**, (11), 1524–1535.
- [6] Maldonado, T.A. Electro-Optic Modulators.
- [7] Courjal, N., Bernal, M.-P., Caspar, A., Ulliac, G., Bassignot, F., Gauthier-Manuel, L. and Suarez, M. (2018) Lithium Niobate Optical Waveguides and Microwaveguides. *Emerging Waveguide Technology*.
- [8] Alferness, R.C. and Buhl, L.L. (1980) Electro-Optic Waveguide TE ↔ TM Mode Converter with Low Drive Voltage. *Optics Letters*, **5**, (11), 473.
- [9] Villa-Manríquez, J.F., Ortiz-Gutiérrez, M., Pérez-Cortés, M., Ibarra-Torres, J.C. and Olivares-Pérez, A. (2017) Holographic Gratings Recorded in PDLC Mixed with Crystal Violet Dye. *Optik*, Elsevier GmbH., **144**, 219–223.
- [10] S, C.R.H., Bunning, T.J., Natarajan, L. V, Tondiglia, V.P. and Sutherland, R.L. (2000) HOLOGRAPHIC POLYMER-DISPERSED LIQUID. 83–115.
- [11] J.A.JENNEY, J. (1970) Holographic Recording with Photopolymers. *Journal of the Optical Society of America*, **60**, (9), 1155–1161.
- [12] Afshari, H., Olyaeefar, B. and Khoshsima, H. (2012) The Refractive Index Grating Formation in Azo Dye Doped Nematic Liquid Crystal. *Molecular Crystals and Liquid Crystals*, **561**, (December), 36–41.
- [13] Pei, Y., Yao, F., Hou, C., Sun, X. and Zhou, Z. (2005) High Diffraction Efficiency and a Quasi-Permanent Grating in Photorefractive Nematic Liquid Crystal at Low Temperature. *Optics letters*, **30**, (6), 631–3.
- [14] d'Alessandro, A., Asquini, R., Gizzi, C., Caputo, R., Umeton, C., Veltri, A. and Sukhov, A. V. (2004) Electro-Optic Properties of Switchable Gratings Made of Polymer and Nematic Liquid-Crystal Slices. *Optics Letters*, **29**, (12), 1405.
- [15] Presnyakov, V., Asatryan, K., Galstian, T. and Chigrinov, V. (2006) Optical Polarization Grating Induced Liquid Crystal Micro-Structure Using Azo-Dye Command Layer. *Optics express*, **14**, (22), 10558–10564.
- [16] Su, W.-C., Huang, C.-Y., Chen, J.-Y. and Su, W.-H. (2010) Effect of Recording-Beam Ratio on Diffraction Efficiency of Polarization Holographic Gratings in Dye-Doped Liquid-Crystal Films. *Optics letters*, **35**, (3), 405–407.
- [17] Marthandappa, M., Somashekar, R. and Nagappa. (1991) Electro-Optic Effects in Nematic Liquid Crystals. *Physica Status Solidi (a)*, **127**, (1), 259–263.
- [18] Tamaoki, N. (2001) Cholesteric Liquid Crystals for Color Information Technology. *Advanced Materials*, **13**, (15), 1135–1147.
- [19] McMillan, W. (1971) Simple Molecular Model for the Smectic A Phase of Liquid Crystals. *Physical Review A*, **4**, (1954), 1238–1246.
- [20] Bezrodna, T., Melnyk, V., Vorobjev, V. and Puchkovska, G. (2010) Low-Temperature Photoluminescence of 5CB Liquid Crystal. *Journal of Luminescence*, Elsevier, **130**, (7), 1134–1141.
- [21] Lebovka, N., Melnyk, V. and Klishevich, G. Low Temperature Phase Transformations in 4-Cyano-4'-Pentylbiphenyl (5CB) Filled by Multiwalled Carbon Nanotubes. (**Lc**), 1–9.
- [22] Khoo, I.-C. (2007) Liquid Crystals. Physics.
- [23] Mykytyuk, Z., Fechan, A., Petryshak, V., Barylo, G. and Boyko, O. (2016) Optoelectronic Multi-Sensor of SO₂ and NO₂ Gases. *Modern Problems of Radio Engineering, Telecommunications and Computer Science, Proceedings of the 13th International Conference on TCSET 2016*, **1**, 402–405.
- [24] Khot, S.A. (2014) Enhancement of Thermal Storage System Using Phase Change Material. *Energy Procedia*, **54**, 142–151.
- [25] Gdovinová, V., Tomašovičová, N., Jeng, S.C., Zakutanská, K., Kula, P. and Kopčanský, P. (2019) Memory Effect in Nematic Phase of Liquid Crystal Doped with Magnetic and Non-Magnetic Nanoparticles. *Journal of Molecular Liquids*, **282**, 286–291.
- [26] Ahmad, F., Jamil, M., Jeon, Y.J., Woo, L.J., Jung, J.E. and Jang, J.E. (2012) Investigation of Nonionic Diazo Dye-Doped Polymer Dispersed Liquid Crystal Film. *Bulletin of Materials Science*, **35**, (2), 221–231.
- [27] Montgomery, G.P., West, J.L. and Tamura-Lis, W. (1991) Light Scattering from Polymer-Dispersed Liquid Crystal Films: Droplet Size Effects. *Journal of Applied Physics*, **69**, (3), 1605–1612.
- [28] Ramanitra, H., Chanclou, P., Vinouze, B. and Dupont, L. (2003) Application of Polymer Dispersed Liquid Crystal (Pdlc) Nematic: Optical-Fiber Variable Attenuator. *Molecular Crystals and Liquid Crystals*, **404**, (1), 57–73.
- [29] De Sio, L., Lloyd, P.F., Tabiryian, N. V. and Bunning, T.J. (2018) Hidden Gratings in Holographic Liquid Crystal Polymer-Dispersed Liquid Crystal Films. *ACS Applied Materials and Interfaces*, **10**, (15), 13107–13112.

- [30] JH-pdics, H.P.L.C., Bunning, T.J., Natarajan, L. V, Sutherland, R.L. and Tondiglia, V.P. (2000) 11 : 1 : Invited Paper : Switchable Reflective Displays Formed From. 121–123.
- [31] Majles Ara, M.H. and Seidali, Z. (2015) The Effect of Sudan Dyes Concentration in the Linear Dichroism of the Nematic Liquid Crystals. *Optik*, Elsevier GmbH., **126**, (2), 297–300.
- [32] Majles Ara, M.H., Mousavi, S.H., Salmani, S. and Koushki, E. (2008) Measurement of Nonlinear Refraction of Dyes Doped Liquid Crystal Using Moiré Deflectometry. *Journal of Molecular Liquids*, **140**, (1–3), 21–24.
- [33] Zolina, V. (1933) FORCES CAUSING THE ORIENTATION OF AN ANISOTROPIC LIQUID .
- [34] B.J. Frisken* and P. Palffy-Muhoray. (1989) Freedericksz Transitions in Nematic Liquid Crystals: The Effects of an in-Plane Electric Field. **40**, (10), 6099–6102.
- [35] Robert H. Chen. (2011) Liquid Crystal Displays Fundamental Physics and Technology. Hoboken, New Jersey.
- [36] Marin, L., Popescu, M.C., Zabolica, A., Uji-I, H. and Fron, E. (2013) Chitosan as Matrix for Bio-Polymer Dispersed Liquid Crystal Systems. *Carbohydrate Polymers*, Elsevier Ltd., **95**, (1), 16–24.
- [37] Ara, M.H.M., Seidali, Z. and Mousavi, S.H. (2010) Electro-Optical Properties of Dye-Doped Nematic Liquid Crystals. *Molecular Crystals and Liquid Crystals*, **526**, 130–138.
- [38] Tumuluri, A., Naidu, K.L. and Raju, K.C.J. (2014). Band Gap Determination Using Tauc 's Plot for LiNbO₃ Thin Films. *Int. J. ChemTech Res*, **6**, (6), 3353–3356.
- [39] Eakin, J.N., Xie, Y., Pelcovits, R.A., Radcliffe, M.D. and Crawford, G.P. (2004). Zero Voltage Freedericksz Transition in Periodically Aligned Liquid Crystals. *Applied Physics Letters*, **85**, (10), 1671–1673.
- [40] Luchetti, L., Gentili, M., Simoni, F., Pavliuchenko, S., Subota, S. and Reshetnyak, V. (2008). Surface-Induced Nonlinearities of Liquid Crystals Driven by an Electric Field. *Physical Review E - Statistical, Nonlinear, and Soft Matter Physics*, **78**, (6).
- [41] Fatriansyah, J.F. and Yusuf, Y. (2009). Dynamic Freedericksz Transition in the Nematic Liquid Crystals Incorporating Elastic Constant k₂₄ Dynamic Freedericksz Transition in the Nematic Liquid Crystals Incorporating Elastic Constant k₂₄. (November).

تحقيق محرز الحيود الكهربائي البصري باستخدام ليزر الهيليوم نيون

عبدالستار احمد عيسى¹ ، Christopher D. Walton²

¹ قسم الفيزياء ، كلية التربية الحويجة ، جامعة كركوك ، كركوك ، العراق

² School of Mathematics and Physical Sciences, University of Hull, UK.

الملخص

تم في هذا البحث انجاز المجال البعيد (Far-Field) لمحزر الحيود الكهربائي البصري (Electro-optical diffraction grating) بالاستفادة من التأثير الكهرو بصري (Electro-optic effect) للبلورات السائلة (Liquid crystal) نوع (5CB). محرز الحيود انجز باستخدام تقاطع حزمتين من اشعة ليزر هليوم نيون ذي الطول الموجي 632.8 نانو متر النافذ من خلال خلية سمكها 5 مايكرون تم ملئها بمحلول البلورات السائلة نوع (5CB) المطعم بصبغة نوع (Sudan Black B (SBB)) وتطبيق مجال كهربائي منتظم على طرفي الخلية. تم تحديد سمك الخلية من خلال استخدام الشريط اللاصق ذو الجانبين سمكه 5 مايكرون حيث تم اعداد عدة خلايا باسماك مختلفة. مختلف التراكيز من صبغة SBB تم اعدادها ودراسة خواصها البصرية. صفر ورتبتين من رتب الحيود تم ملاحظتها اثناء التجربة حيث تم التحقق من وجودها باستخدام اشعة ليزر هليوم نيون اخر باقل طاقة. 16 مايكرون المسافة بين رتب محرز الحيود المنجز (Grating period) تم قياسها عمليا. تم التحقق من تأثير تغيير الفولتية على انجاز محرز الحيود الكهربائي البصري. تم التحقق تجريبيا من امكانية انتاج محرز الحيود الكهربائي البصري باستخدام خلية ملئت بمحلول يتكون من البلورات السائلة (5CB) مطعمة بصبغة SBB والبوليمر الحيوي (Chitosan) وذلك لتعزيز خاصية الامتصاص البصري للمحلول. مختلف الاجهزة تم استخدامها لغرض دراسة وتحليل النتائج التي تم الحصول عليها تجريبيا : المجهر الاليكتروني الماسح (Scanning Electron Microscopy (SEM) , مجهر القوة الذري (Atomic Force microscopy (AFM) , المجهر الضوئي و مقياس الطيف الضوئي للاطوال الموجية المرئية وال فوق البنفسجية. تمت الدراسة العملية لمحزر الحيود الكهربائي البصري والذي تم انجازه. تم وباختصار مناقشة بعض التطبيقات العملية للبلورات السائلة وكذلك التطبيقات العملية الخاصة بالتأثير الكهرو بصري.